System analysis of the functional cross-talk between PPARalpha, LXR and FXR in the human HepaRG liver cells

Leonore Wigger[1,2,a], Cristina Casals-Casas[3,a], Michaël Baruchet[3], Khanh B. Trang[3], Sylvain Pradervand[1,2], Aurélien Naldi[3,b] and Béatrice Desvergne[3,b]
[1]Lausanne Genomic Technologies Facility, Center for Integrative Genomics, University of Lausanne, Switzerland
[2]Vital-IT, Swiss Institute of Bioinformatics, Lausanne, Switzerland
[3]Center for Integrative Genomics, University of Lausanne, Switzerland

[a] The two first authors contributed equally
[b] Corresponding authors: Beatrice.Desvergne@unil.ch and aurelien.naldi@gmail.com

Keywords : Nuclear receptors, cell-cycle, network, metabolism, liver cells

Abstract

Transcriptional regulations exert a critical control of metabolic homeostasis. In particular, the nuclear receptors (NRs) are involved in regulating numerous pathways of the intermediate metabolism. The purpose of the present study was to explore in liver cells the interconnectedness between three of them, LXR, FXR, and PPARα, all three known to act on lipid and glucose metabolism, and also on inflammation. The human cell line HepaRG was selected for its best proximity to human primary hepatocytes. Global gene expression of differentiated HepaRG cells was assessed after 4 hours and 24 hours of exposure to GW3965 (LXR agonist), GW7647 (PPARα agonist), and GW4064 and CDCA (FXR synthetic and natural agonist, respectively). Our work revealed that, contrary to our expectations, NR specificity is largely present at the level of target genes, with a smaller than expected overlap of the set of genes targeted by the different NRs. It also highlighted the much broader activity of the synthetic FXR ligand compared to CDCA. More importantly, our results revealed that activation of FXR has a pro-proliferative effect and decreases polyploidy of hepatocytes, while LXR inhibits the cell cycle progression, inducing hepatocyte differentiation and a higher polyploidism. Conclusion: these results highlight the importance of analyzing the different NR activities in a context allowing a direct confrontation of each receptor outcome, and reveals the opposite role of FXR and LXR in hepatocyte cells division and maturation.

Introductory statement

Homeostasis of energy metabolism results in a steady-state output of energy available for cell functions, despite the discontinuity of food intake and activities. Metabolic regulation in the liver is a major component of energy homeostasis. At the molecular level, metabolic regulation relies on three main types of control: allosteric, post-translational, and transcriptional. While most metabolic regulations benefit from a coordination of these mechanisms, transcriptional regulation exerts a critical control for keeping each component of the regulatory mechanisms at appropriate operating levels.
Nuclear receptors (NRs) are transcription factors that share many structural properties, notably a DNA binding domain folded in two zinc fingers and a ligand-binding pocket made of 13 alpha helices. Within the superfamily of NRs, which encompasses 48 members in Humans, there is a sub-class called metabolic sensors. They are bound and activated by

endogenous ligands that are metabolites belonging to the intermediary metabolisms, and actively contribute to the regulation of metabolic pathways. The discovery of each receptor initially emphasized the specificity of each receptor in a given metabolic pathway, for example the peroxisome proliferator-activated receptors (PPARα , PPARβ/δ , PPARγ ; NRC1, NRC2, and NRC3, respectively in the international nomenclature) in lipid metabolism, the farnesoid X receptors (FXR and FXRβ; NR1H4 and NR1H5P, respectively) in bile acid metabolism, and the liver X receptor (LXRα and LXRβ; NR1H3 and NR1H2, respectively) in cholesterol metabolism (1, 2). However the classical linear view with each NR engaged in modulating one or a few pathways is challenged by the numerous and complex interconnections between the metabolisms of glucides, lipids and amino acids, as well as by the numerous roles of NRs outside of metabolism. This highlights the need to delineate the regulatory network underlying homeostasis through systemic approaches.

The aim of this study was to explore the connections between the three NRs mentioned above. More specifically, PPARα is activated by unsaturated fatty acids and involved in many facets of both lipid and glucose metabolism. LXRα and LXRβ are activated by cholesterol derivatives, but are also strongly lipogenic. Finally, FXR is bound by bile acids and is considered as a critical regulator of cholesterol metabolism (3). Thus, they clearly affect overlapping pathways. To better explore the interconnections, one must first assess the activity of each receptor in a given common and reproducible cellular context. For that purpose, we used the HepaRG hepatocarcinoma cell line, introduced in 2002 by Gripon et al. (4). HepaRG cells have been described as the closest in vitro model to human liver metabolism (5) and as a strong candidate for bioartificial liver applications (6).

Our work revealed that, in contrast to our expectations, NR specificity is largely present at the level of target genes, with a smaller than expected overlap of the set of genes targeted by the different NRs. The connection and coordination then mainly occur at the level of pathways. Importantly, our observations also highlight an important role of FXR and LXR in regulating cell growth and death of liver cells, with opposite effects on cell cycle progression and on hepatocyte polyploidization.

Material and Methods

Cell culture and chemicals

Cultures of HepaRG cells, generously provided by C. Guguen-Guillouzo, were grown as described in details in (4). After differentiation, hepatocyte-like cells were enriched by selective detachment using mild trypsinization and plated at 1.5x10-5/cm2 density in complete media plus 2% DMSO as described in (7). Based on pilot experiments, 2 µM for GW3965 (called LXR-L in this study), 1 µM for GW4064 and GW7647 (FXR-L and PPARa-L in this study) and 50 µM for CDCA were used. All compounds were diluted in DMSO, which was also used as vehicle control. The different agonists and CDCA were purchased from Sigma-Aldrich (St. Louis, MO).

RNA extraction and Quantitative RT–PCR

Total RNA from cell culture was extracted with Trizol Reagent (Life Technologies, Carlsbad, CA), following the manufacturer's instructions. The PCR arbitrary units of each gene were defined as the mRNA levels normalized to the *GAPDH* and the *EEF1A1* expression level in each sample using the qBase Software. The primers sequences are available upon request.

Microarrays

Microarrays were prepared from two time points, 4 hours and 24 hours, with 18 samples per time points: 3 samples of each of the 6 condition, i.e. FXR-L, LXR-L, PPARa-L, CDCA, vehicle controls (DMSO) and untreated controls. Samples were hybridized to Affymetrix GeneChip Human Gene 1.0 ST arrays (Affymetrix, Santa Clara, CA). Data summarisation and normalization was performed on all 36 samples together, using the robust multichip analysis (RMA) algorithm implemented in the Affymetrix Expression Console software. Probe sets that could not be mapped to any gene symbol were discarded. When more than one probe set was associated with the same gene symbol, only the probe set with the highest variance across the normalized expression levels in the 18 arrays from time point 4h was retained in the data set. After these two filtering steps, 20270 genes remained. Microarray data are available on GEO (accession number GSE124053).

Differential Gene (DE) Expression

Differential gene expression for each treatment at each time point was analyzed with moderated t-tests performed with the bioconductor package LIMMA (8). (See supplemental material for a detailed method). The resulting gene lists (limma output) are available in the supplementary data archive data_and_code.zip.

Gene Set Enrichment Analysis (GSEA)

Gene set enrichment analysis (GSEA) was performed as described in (9) for each treatment at each time point. Most of the gene sets were taken from KEGG, while BIOCARTA sets from the Broad Institute's Molecular Signatures Database (MsigDB version 3.0: www.broadinstitute.org/gsea/msigdb) are explicitly mentioned. We considered a gene set potentially enriched if it had an adjusted p-value lower than 0.2. The leading edge subsets of significantly enriched pathways were extracted, using the GSEA algorithm (see supplemental materials for a detailed method). The resulting pathway lists are available in the supplementary data archive supplementary_archive.zip.

Cell-cycle analysis

As described in (10), cells were fixed in 70% ice-cold ethanol, washed in PBS and re-suspended in staining solution containing 20 µg/ml propidium iodide, 0.05% Triton X-100 and 200 µg/ml RNAse A (Sigma-Aldrich, St. Louis, MO) and 10,000 cells were analyzed per sample using the BD bioscience FACSDiva. Data were based on 8 replicates from 3 independent experiments.

Western Blot

SDS-PAGE was performed using cultured HepaRG cell extracts and transferred to nitrocellulose membranes (Novex, Life Technologies, Carlsbad, CA). After blocking, bands were detected with primary antibodies to p27 (#2552), CCND3 (#2936) and RB (RB Antibody Sampler Kit #9969) and secondary antibodies, anti-rabbit (#7074) or anti-mouse (#7076) IgG conjugated to horseradish peroxidase (Cell Signaling Technology Inc., Danvers, MA), and applying the SuperSignal® West Pico Chemiluminescent Substrate (Thermo Fisher Scientific, Bremen, Germany). Membranes were then exposed to x-ray films (GE Healthcare, Milwaukee, WI). Beta-actin (#A2228, Sigma-Aldrich, St. Louis, MO) was used as a loading control.

Results

Defining and validating the experimental set-up

The aim of the experiment was to evaluate which hypothesis could best explain the cross-regulatory action of the nuclear receptors on metabolic pathways. Do the receptors regulate common target genes, or do they regulate different sets of genes belonging to common pathways?

Differentiated HepaRG cells were chosen since their global gene expression patterns are much closer to liver or primary human hepatocyte cultures than the widely used HepG2 cell line (5) and include the expression of PPARα, LXRα/β, and FXR at mRNA levels. This expression is consistent with that observed in human primary cells. To activate each receptor, we used synthetic ligands known to be the most specific: GW4064 for FXR, GW3965 for LXRs, and GW7647 for PPARα, hereafter called FXR-L, LXR-L, and PPARa-L. We also used the bile acid CDCA, which is a natural ligand of FXR (11, 12). CDCA is also known to affect LXR (13), PPARα (14) and HNF4 (15) pathways, even though the mechanisms are not yet well understood. For each compound, we selected the lowest concentration that triggered a good response of canonical targets in a pilot experiment (data not shown).

Microarrays were run first on differentiated HepaRG, prior any treatment. A second batch of microarrays was then run 4 hours after the beginning of the cell exposure to each treatment, in order to identify direct target genes, whereas the last batch of microarrays, run at 24h, aimed at identifying global crosstalk. These analyses confirmed that the NRs of interest were expressed in HepaRG cells.

We then identified all genes differentially expressed, when compared to the group of control samples, in at least one of the treatment conditions at either of the two time points. We used the RNA datasets of differentially expressed genes as features to perform a hierarchical clustering of the five different models analyzed by Hart *et al*. (5). As shown in supplemental Figure 1, the profile of our set of DE genes was found to be similar in human liver and in primary hepatocytes, whereas HepG2 cells have a gene expression pattern far from all the other models analyzed. The expression profile of HepaRG cells (differentiated and undifferentiated) was distinct from that of liver cells, but much closer to it than that of HepG2 cells.

Altogether, these initial observations confirmed that HepaRG cells are in this context more pertinent than other in vitro models widely used in literature, such as HepG2 cells (16, 17).

NR cross-talks happen at the pathway level and are mostly related to metabolism

The analyses of the set of genes differentially expressed at the 4 hours time point identified 681 differentially expressed genes, comparing the control to each of the treatments. A good part of these genes are associated to the FXR-L treatment (~500 genes) and to a lesser extent to CDCA (~160 genes), while fewer are associated to PPARa-L (~90), and to LXR-L (<10) (Fig 1A, left part). This important variation in the number of genes modulated by each treatment is consistent with separate gene expression or ChIP-seq studies (18-20). These differentially expressed genes include the main known targets of the selected nuclear receptors. For example, FXR-L and CDCA modulate *ABCB11* (*BSEP*), *ABCB4* (*MDR3*), *CYP7A1* and *PPARGC1* expression. Some known FXR target genes are found modulated only by FXR-L, and not by CDCA, like *NR0B2* (*SHP*), *HNF4A* and *PPARA*. Others were only regulated by CDCA like *UGTB4*, *RORA*, *HMGCS1* and *NR1D1*/2. PPARa-L up-regulates its well-established target genes *FABP4*, *HMGCS2*, *ACOX1*, *CD36* and *CPT1A*. At this point, LXR-L has a very modest effect, modulating less than 10 genes, which include known LXR target genes *SCD*, *SREBF1* (also called *SREBP)*, *ABCA1*, *FASN*, and *MYLIP/IDOL*.

We then identified 1611 differentially expressed genes at the 24h time-point (Fig 1A, right part). This strong increase compared to the early time-point is consistent with the identification of indirect effects. For example, *SHP* (*NR0B2*), a well-described FXR target gene very significantly increased at 4 hours by FXR-L, mediates indirect regulations, such as the strong down-regulation of Cyp7A1 seen at 24h (21). Also, SREBP1c, which is induced by LXR at 4h, is a regulator of key genes in lipid metabolism (22). These genes are in turn induced at 24h, as for example *SCD1*, *ACLS1* and *HMGCR* and *HMGCS*. Like at 4h, most genes were associated to FXR-L (~1100) and CDCA (~350) and fewer to PPARa-L (~140) and LXR-L (<50).

Intriguingly, less than half of the genes identified at 4h were still differentially expressed at 24h (312 out of 681) (Table 1), suggesting that most direct effects are only transient. Comparing the different treatments shows surprisingly few crosstalks at the level of transcriptional regulation: among the 1980 differentially expressed genes, 75% are specific to a single treatment. As expected, FXR-L and CDCA have the biggest overlap, sharing 63% of the common genes (16% of all the differentially expressed ones). Nevertheless some genes are common targets for different NRs. For example *PDK4*, *HMGCS2*, and *ACOX1*, involved in lipid metabolism, are all up-regulated by PPARa-L and down-regulated by FXR-L; *ABCA1* and *MYLIP*, well described target genes of LXR (3, 23) are also down-regulated by FXR. Some other genes involved in lipid and glucose metabolism like, for example, *FASN*, *FABP4*, *LPL*, *INSIG1*, *SCD,* are found up-regulated both by PPARa-L and LXR-L (Fig. 1A and Table 1).

To explore the possibility of crosstalk at the level of pathways, we looked for enriched pathways shared across time-points and treatments. We identified 153 enriched pathways in our dataset. Like for differentially expressed genes, we observed an increase in the number of enriched pathways between the early and late time-points. Most enriched pathways (54%) were identified at both time-points (compared to 16% of the differentially expressed genes). Even though they remain predominantly associated to the FXR-L (140) or CDCA (114) treatments, PPARa-L (62) and LXR-L (46) treatments are also well represented. Importantly, 80% (123/156) of the enriched pathways are shared between several treatments, compared to 25% (500/1980) at the gene level. While 40 of the 123 shared pathways are still specific to the related FXR-L and CDCA treatments, which both target the same NR, the remaining 83 pathways are associated with two or even three treatments targeting separate NRs and thus point to crosstalk at the pathway level. In other words, more than half of all enriched pathways (83/153) are associated with at least two NRs (Figure 1B; Table 1).

The most striking observation at this point is that few genes are co-regulated by the NRs studied herein. In contrast, the cross-talk appeared in the associated pathways. We therefore explored further the shared enriched pathways to discover new NR crosstalks.

Cell growth and death is overrepresented in FXR and LXR cross-talks

Based on the KEGG pathway database (www.genome.jp/kegg/pathway.html), we manually classified enriched pathways into 4 groups: “Metabolism”, “Cell Growth and Death”, “Immune System” and “Other”. ‘Transport and catabolism’, ‘Endocrine, Digestive, Excretory Systems’ and ‘Endocrine and Metabolic diseases’ were merged into the 'Metabolism' group. ‘Genetic Information Processing’, ‘Cellular Processes’ (other than ‘Peroxisome’) and ‘Cancers’ form the ‘Cellular Growth and Death’ group. Finally, ‘Immune and Infectious Diseases’ correspond to our ‘Immune System’ group. Unclassified pathways that we could not associate to one of these 3 groups form the ‘Other’ group (the names of the pathways in each category are made available in the supplementary archive "data_and_code.zip").

As a set of core genes may drive different pathways belonging to the same group, we then counted the genes belonging to the leading edge of the GSEA curves and involved in several

pathways within each group (illustrated in supplementary Figure S2). In the metabolism group, only 14 genes are involved in at least 10% of the pathways. This amount increases for the two other groups with 121 genes being involved in at least 10% of pathways of cell growth and death and 96 for the immune system; 37 of them are common to both groups. As most DE genes are specific to one pathway, we are confident about the relevance of the enriched pathways. This analysis thus confirmed that metabolic regulations, which are the main functions of the NRs, are represented by the largest group of enriched pathways with the highest specificity of involved genes.
The 'Metabolism' group covers 48% of the enriched pathways, 'Cellular Growth and Death' cover 30%, and 'Immune System' 14%. Unsurprisingly, all pathways shared by the three NR and 65% of the ones shared by FXR and PPARα are involved in metabolism (Table 2). However, 72% of the pathways associated to both FXR-L and LXR-L are related to cell growth and death, while this group does not represent more that 30% in the other combinations of treatments. The role of FXR and LXR in liver is considered as mostly related to metabolism regulation with main roles in lipid, cholesterol and glucose metabolism, FXR being anti-lipogenic and LXR pro-lipogenic (1). However they also play an important role in liver regeneration (24-28) or cancer development (29-31).

FXR and LXR oppositely regulate the cell cycle progression

To understand the mechanisms involving FXR and LXR in the regulation of cell growth and death, we focused on the "Cell cycle" pathway, which is enriched in four conditions: at 4h by FXR-L and CDCA, and at 24h by FXR-L and LXR-L. We further looked at the genes that belong to the leading edges of the cell cycle pathway at 24h for FXR-L (45 genes) and LXR-L (41 genes). Intriguingly, FXR-L predominantly activates gene expression while LXR-L inhibits it. Twenty-three of the 26 genes found in the leading edges for both treatments are oppositely regulated by FXR-L and LXR-L (Fig. 2).
Using the KEGG diagrams to illustrate the corresponding pathway and genes (Fig. 3 and supplementary Fig. S3), the patterns of FXR-L at 4h show an up-regulation of genes involved in the G1/S transition like *C-MYC*, and *CCND1*. At 24h, the cell cycle key players are upregulated by FXR-L and downregulated by LXR-L. The list comprises *CCNE*, *CDK2*, and *P18* as well as genes involved in DNA replication such as *CDC6* and members of the minichromosome complex (*MCM*) (32, 33). These observations suggest a pro-proliferative role for FXR, with an up-regulation of genes involved in the G1/S progression at 4h and a more global positive regulation at 24h. LXR have the opposite effect inhibiting genes involved in the cell cycle progression and DNA replication.

To determine if these gene modulations reflect an actual regulation of the cell cycle, we analyzed the distribution of cell cycle phases by propidium iodide staining and flow cytometry. We treated HepaRG cells with FXR-L and LXR-L for 24, 48 or 72 hours. Knowing the pro-proliferative effect of serum in the culture media, the experiment was made both in the presence and in the absence of serum. Flow cytometry analyses revealed two well separated populations corresponding to diploid and tetraploid populations (2C and 4C DNA content, respectively), characteristic of mammalian hepatocytes (Fig. 4A) (34).
In serum free conditions, FXR-L treatment triggered a decrease of the tetraploid cell population, visible at 24h and significant at 48h and 72h, with 25% and 36% less 4C cells respectively, while LXR-L treatment has no significant effect (Fig. 4D). In presence of serum, the 4C population also decreases at 72h with FXR-L (22%), whereas it significantly increases with LXR-L (17%).
The mechanisms involved in the mammalian hepatocyte polyploidism are not yet well understood. However polyploidy is known to appear at the terminal differentiation during late

foetal development, while proliferating cells are mainly diploid. Indeed, by sorting the cells by their cell cycle phase status, we observe in the diploid population an accumulation of cells at G1 after 48 hours treatment with LXR-L (suppl. Fig. S5). This accumulation is further increased at 72 hours, while S and G2 populations are decreasing (Fig. 4B). In opposite manner, FXR-L tends to decrease the G1 population and increase the S and G2 populations at 24h, even if these changes are statistically significant only at 72h in serum-free conditions (Fig. 4B and suppl. Fig. S5). The tetraploid population shows the same pattern with a stronger effect of FXR-L, decreasing significantly the G1 population in both conditions (Fig. 4C).
Hence, our results are consistent with a correlation between polyploidy and hepatocyte differentiation stage (35): FXR-L has a pro-proliferative effect and decreases polyploidy, while LXR-L inhibits the cell cycle progression, inducing hepatocyte differentiation and a higher polyploidism.
Positionning the genes identified in the GSEA results with the BIOCARTA pathways show that FXR-L affects the G1/S and G2/M checkpoints, while LXR-L only affects the G1/S checkpoint, blocking the cells in the G1 phase (Fig. 4). To better assess the key players involved in these regulations, we evaluated the activity of some cell cycle regulators at the transcriptional and post-transcriptional levels (Fig. 5). The LXR-L treatment affects the G1/S checkpoint by inhibiting the expression of *CDC25A* and *CCNE2*, and upregulating the expression *CDKN2B* (p15). Quantitative PCR also shows a downregulation of *E2F1* and *E2F2* mRNA expression by qPCR (Fig. 5A). The treatment also has effects at the post-transcriptional level inhibiting the CCND3 (Cyclin D3) expression and decreasing RB phosphorylation (Fig. 5B&C). On the other hand, FXR-L also deeply affects the key players of the G1/S checkpoint, *CCNE1* and *SKP2,* which are upregulated by FXR-L (Fig. 5A). This is consistent with the observed hyper-phosphorylation of RB (Fig. 5B&C) and should result in an activation of the cell cycle progression. Finally, FXR-L also affects the mRNA expression of the G2/M checkpoint regulators *CDC25C* or *CCNA2* (Fig. 5A).

Discussion

Nuclear receptors are important transcriptional regulators of metabolism (2), acting on both specific and shared pathways. The numerous side effects associated to novel therapeutics for metabolic disorders based on NRs activation or inhibition highlight the need for understanding their regulatory crosstalks. Herein, we demonstrated that the cross-talk between the three selected receptors, FXR, LXR and PPARα is largely due to a distribution of their respective specific target genes in shared pathways, rather than to their effects on common genes. This study further allowed identifying an important role of FXR and LXR in controlling, in opposite manner, some key factors of cell cycle progression in liver cells and of hepatocyte polyploidization.
A strength of this study is the use of HepaRG cells, which exhibit a gene expression profile close to the primary human cells. By using a simplified, well standardized, and human-related model, the results obtained are likely to be informative with respect to human responses to the ligands used herein. Another strength of this study was to obtain the profile of gene expression upon activation of FXR, LXR and PPARα, respectively, using the very same experimental conditions. This was the condition to be able to interpret the specificity of each receptor. Indeed, existing gene expression profiles for these receptors that have already been published in the GEO repository cannot be directly compared due to experimental setups and cell line (for example, HepG2 vs HepaRG, vs primary hepatocytes, see (5) and Suppl. Fig. S1).

An important observation in the present study is that the three receptors we tested regulate relatively few genes in common. There are several levels of promiscuousness between NRs: they share the same binding partner RXR, they have promiscuous binding sites, and they act on common metabolic pathways. However, our results emphasize their specificity in activating genes. This specificity does apply at the very early time point (4h), where we expect only direct target genes to be activated, but also extend to the late time point (24h), where new genes are activated, in part as a consequence of the first set of gene activation. Similar observations have been reported when analyzing the gene regulatory profile of PPARγ and LXR receptors in cancer cells. While they both exert an inhibitory action on cancer cell proliferation, via a common metabolic reprogramming, the genes they activated remain specific to each receptor (36).

Another feature of interest is the overlap but also specificity of the action of CDCA and FXR-L. CDCA is considered to be a natural ligand for FXR (11). However, a large number of genes are activated with the synthetic ligand but not with the natural one. This may be explained by the so-called selective NR modulator effect (37), by which the conformational changes that occur in NRs upon ligand binding may provoke a different interface for co-factor recruitment, depending on the nature of the ligand. It may also be caused by a different affinity of the ligand, a different accessibility, and/or different metabolism of the ligand within the cell. These facts are particularly important when searching for appropriate ligands aimed at therapeutic usage, implying that a full exploration of the gene expression profile for each new molecule proposed is required.

Unsurprisingly, the main pathways enriched by the three NR agonists are related to metabolism. More interestingly, 72% of the pathways shared by FXR and LXR are involved in regulations of cell growth and death. In addition, 56% of genes belonging to the leading edge of the cell cycle pathway (evaluated by GSEA) are common to both NRs but with an opposite modulation. The anti-proliferative activities of LXR has been observed in a number of cellular systems, including vascular smooth muscle cells, cancer cells, T lymphocytes, pancreatic islet beta cells and mouse liver (Reviewed in (38)). This brought up the claim that LXR might be a target for anti-tumoral treatments in different tissues, mainly documented in breast, prostate and intestinal cancer cells. LXR mediated cell-cycle inhibition has been mechanistically correlated with the expression of lipogenic and triglyceride accumulation (31), but could also be related to the inhibition of SKP2 transcription (33, 39). In the present study, SKP2 is not affected by LXR-L, suggesting that LXR's anti-proliferative activity is due to alternative mechanisms, such as LXR-mediated repression of AP1 signaling (36, 40).

The role of FXR is more controversial, or complex. FXR was demonstrated to be involved in the bile-acid dependent progression of intestinal metaplasia (41, 42), possibly through a SHP-dependent increase of CDX2 gene expression (43). In contrast, the deletion or down-regulation of FXR favors hepatocarcinogenesis (29, 44, 45), suggesting that FXR plays a protective role. Finally, FXR is also required for liver regeneration (25, 28, 46). The mechanism by which FXR can both favor liver regeneration and protect from hepatocarcinogenesis remains unsettled (44). The following three main findings of the present study are noteworthy in this context. First, FXR-L significantly upregulates IL6 and increases the expression of a number of pro-inflammatory cytokines, such as *IL1b*, *CSF1*, *CSF2*, and *TGFb3*. These signals are indeed important in triggering the early response for liver regeneration (44), even though these results are in contradiction with the reported anti-inflammatory activities of FXR, via down-regulation of the NF-KB pathway (47), not observed in our dataset. Second, we showed the positive effect of FXR on cell cycle progression, increasing the activities of key regulators of the G1/S and G2/M checkpoints. Third, we show that FXR-L inhibits hepatocyte polyploidization. This effect could involve the insulin-signaling pathway, which is sitting at the cross-road of many metabolic pathways, and

contributes to the formation of binucleated tetraploid liver cells through the PI3K/Akt pathway (48). Indeed, the insulin pathway is affected by all treatments in this study, but more particularly by FXR-L at 24h (p-value<0.001), with an inhibition of 17 key genes including INSR, IRS and PI3K (Suppl. Fig. S4). This suggests that FXR may prevent the polyploidization of the HepaRG cells via inhibition of the insulin INSR/PI3K pathway.. Interestingly, polyploidy was shown to trigger cell transformation and tumor formation in p53-null cells (49). Albeit it remains difficult to generalize this observation to other cellular context, the inhibition of polyploidization mediated by FXR-L may contribute to its protective role against carcinogenesis.

Thus, besides illustrating the high levels of target gene specificity of each NR tested herein, our results revealed an important antagonistic effect of FXR and LXR on cell cycle progression in hepatocytes. Assessing these roles in different cells and tissues might be of importance when contemplating the therapeutic applications that these two receptors are conveying.

Acknowledgements

We thank Frédéric Schütz and Thierry Sengstag for making their unpublished R package for gene set enrichment analysis (mygsea2) available, and we are grateful to Frédéric Schütz for excellent input on how to choose parameter settings. Particular thanks go to Christiane Guguen-Guillouzo and its laboratory for the generous gift of HepaRG cells and shared information on their maintainance. The Genomic Technologies Facility of the University of Lausanne has realized all the microarrays including data normalization.

Financial support

This study was supported by the État de Vaud, FNRS (grant 31003A_135583/1 and 310030_156771/1; BD), CC was further supported by a Novartis grant, and BD by FP7 NR-NET (606806).

Author's contributions

LW: performed data analysis (microarray data processing, differential expression analysis, GSEA), coordinated the author's tasks, edited the manuscript, tables and figures. CCC: contributed to conceive the study design, performed the wet-lab experiments, wrote the first draft of the manuscript, edited the manuscript, and constructed the tables and figures. MB contributed to the experimental work and edited the manuscript. KBT contributed to data analyses and edited the manuscript. SP supervised bioinformatics analyses and edited the manuscript. AN conceived the study design, supervised the bioinformatics, performed the network analyses, wrote the first draft of the manuscript, created and edited the figures and tables, and edited the manuscript. BD conceived the study and the study design, supervised and coordinated the dual experimental and bioinformatics approaches, wrote and edited the manuscript.

References

1. Francis GA, Fayard E, Picard F, Auwerx J. Nuclear receptors and the control of metabolism. Annu Rev Physiol 2003;65:261-311.
2. Desvergne B, Michalik L, Wahli W. Transcriptional regulation of metabolism. Physiol Rev 2006;86:465-514.
3. Calkin AC, Tontonoz P. Transcriptional integration of metabolism by the nuclear sterol-activated receptors LXR and FXR. Nat Rev Mol Cell Biol 2012;13:213-224.

4. Gripon P, Rumin S, Urban S, Le Seyec J, Glaise D, Cannie I, Guyomard C, et al. Infection of a human hepatoma cell line by hepatitis B virus. Proc Natl Acad Sci U S A 2002;99:15655-15660.
5. Hart SN, Li Y, Nakamoto K, Subileau EA, Steen D, Zhong XB. A comparison of whole genome gene expression profiles of HepaRG cells and HepG2 cells to primary human hepatocytes and human liver tissues. Drug Metab Dispos 2010;38:988-994.
6. Nibourg GA, Chamuleau RA, van der Hoeven TV, Maas MA, Ruiter AF, Lamers WH, Oude Elferink RP, et al. Liver progenitor cell line HepaRG differentiated in a bioartificial liver effectively supplies liver support to rats with acute liver failure. PLoS One 2012;7:e38778.
7. Cerec V, Glaise D, Garnier D, Morosan S, Turlin B, Drenou B, Gripon P, et al. Transdifferentiation of hepatocyte-like cells from the human hepatoma HepaRG cell line through bipotent progenitor. Hepatology 2007;45:957-967.
8. Smyth GK. Linear models and empirical bayes methods for assessing differential expression in microarray experiments. Stat Appl Genet Mol Biol 2004;3:Article3.
9. Subramanian A, Tamayo P, Mootha VK, Mukherjee S, Ebert BL, Gillette MA, Paulovich A, et al. Gene set enrichment analysis: a knowledge-based approach for interpreting genome-wide expression profiles. Proc Natl Acad Sci U S A 2005;102:15545-15550.
10. Landry S, Narvaiza I, Linfesty DC, Weitzman MD. APOBEC3A can activate the DNA damage response and cause cell-cycle arrest. EMBO Rep 2011;12:444-450.
11. Parks DJ, Blanchard SG, Bledsoe RK, Chandra G, Consler TG, Kliewer SA, Stimmel JB, et al. Bile acids: natural ligands for an orphan nuclear receptor. Science 1999;284:1365-1368.
12. Kawamata Y, Fujii R, Hosoya M, Harada M, Yoshida H, Miwa M, Fukusumi S, et al. A G protein-coupled receptor responsive to bile acids. J Biol Chem 2003;278:9435-9440.
13. Talukdar S, Bhatnagar S, Dridi S, Hillgartner FB. Chenodeoxycholic acid suppresses the activation of acetyl-coenzyme A carboxylase-alpha gene transcription by the liver X receptor agonist T0-901317. J Lipid Res 2007;48:2647-2663.
14. Pineda Torra I, Claudel T, Duval C, Kosykh V, Fruchart JC, Staels B. Bile acids induce the expression of the human peroxisome proliferator-activated receptor alpha gene via activation of the farnesoid X receptor. Mol Endocrinol 2003;17:259-272.
15. Li T, Jahan A, Chiang JY. Bile acids and cytokines inhibit the human cholesterol 7 alpha-hydroxylase gene via the JNK/c-jun pathway in human liver cells. Hepatology 2006;43:1202-1210.
16. Samanez CH, Caron S, Briand O, Dehondt H, Duplan I, Kuipers F, Hennuyer N, et al. The human hepatocyte cell lines IHH and HepaRG: models to study glucose, lipid and lipoprotein metabolism. Arch Physiol Biochem 2012;118:102-111.
17. Rogue A, Lambert C, Josse R, Antherieu S, Spire C, Claude N, Guillouzo A. Comparative gene expression profiles induced by PPARgamma and PPARalpha/gamma agonists in human hepatocytes. PLoS One 2011;6:e18816.
18. Boergesen M, Pedersen TA, Gross B, van Heeringen SJ, Hagenbeek D, Bindesboll C, Caron S, et al. Genome-wide profiling of liver X receptor, retinoid X receptor, and peroxisome proliferator-activated receptor alpha in mouse liver reveals extensive sharing of binding sites. Mol Cell Biol 2012;32:852-867.
19. Thomas AM, Hart SN, Kong B, Fang J, Zhong XB, Guo GL. Genome-wide tissue-specific farnesoid X receptor binding in mouse liver and intestine. Hepatology 2010;51:1410-1419.

20. van der Meer DL, Degenhardt T, Vaisanen S, de Groot PJ, Heinaniemi M, de Vries SC, Muller M, et al. Profiling of promoter occupancy by PPARalpha in human hepatoma cells via ChIP-chip analysis. Nucleic Acids Res 2010;38:2839-2850.
21. Goodwin B, Jones SA, Price RR, Watson MA, McKee DD, Moore LB, Galardi C, et al. A regulatory cascade of the nuclear receptors FXR, SHP-1, and LRH-1 represses bile acid biosynthesis. Mol Cell 2000;6:517-526.
22. Repa JJ, Liang G, Ou J, Bashmakov Y, Lobaccaro JM, Shimomura I, Shan B, et al. Regulation of mouse sterol regulatory element-binding protein-1c gene (SREBP-1c) by oxysterol receptors, LXRalpha and LXRbeta. Genes Dev 2000;14:2819-2830.
23. Zelcer N, Hong C, Boyadjian R, Tontonoz P. LXR regulates cholesterol uptake through Idol-dependent ubiquitination of the LDL receptor. Science 2009;325:100-104.
24. Chen WD, Wang YD, Zhang L, Shiah S, Wang M, Yang F, Yu D, et al. Farnesoid X receptor alleviates age-related proliferation defects in regenerating mouse livers by activating forkhead box m1b transcription. Hepatology 2010;51:953-962.
25. Huang W, Ma K, Zhang J, Qatanani M, Cuvillier J, Liu J, Dong B, et al. Nuclear receptor-dependent bile acid signaling is required for normal liver regeneration. Science 2006;312:233-236.
26. Lo Sasso G, Celli N, Caboni M, Murzilli S, Salvatore L, Morgano A, Vacca M, et al. Down-regulation of the LXR transcriptome provides the requisite cholesterol levels to proliferating hepatocytes. Hepatology 2010;51:1334-1344.
27. Borude P, Edwards G, Walesky C, Li F, Ma X, Kong B, Guo GL, et al. Hepatocyte-specific deletion of farnesoid X receptor delays but does not inhibit liver regeneration after partial hepatectomy in mice. Hepatology 2012;56:2344-2352.
28. Chen WD, Wang YD, Meng Z, Zhang L, Huang W. Nuclear bile acid receptor FXR in the hepatic regeneration. Biochim Biophys Acta 2011;1812:888-892.
29. Kim I, Morimura K, Shah Y, Yang Q, Ward JM, Gonzalez FJ. Spontaneous hepatocarcinogenesis in farnesoid X receptor-null mice. Carcinogenesis 2007;28:940-946.
30. Chuu CP, Lin HP. Antiproliferative effect of LXR agonists T0901317 and 22(R)-hydroxycholesterol on multiple human cancer cell lines. Anticancer Res 2010;30:3643-3648.
31. Kim KH, Lee GY, Kim JI, Ham M, Won Lee J, Kim JB. Inhibitory effect of LXR activation on cell proliferation and cell cycle progression through lipogenic activity. J Lipid Res 2010;51:3425-3433.
32. Mendez J, Stillman B. Chromatin association of human origin recognition complex, cdc6, and minichromosome maintenance proteins during the cell cycle: assembly of prereplication complexes in late mitosis. Mol Cell Biol 2000;20:8602-8612.
33. Blaschke F, Leppanen O, Takata Y, Caglayan E, Liu J, Fishbein MC, Kappert K, et al. Liver X receptor agonists suppress vascular smooth muscle cell proliferation and inhibit neointima formation in balloon-injured rat carotid arteries. Circ Res 2004;95:e110-123.
34. Celton-Morizur S, Merlen G, Couton D, Desdouets C. Polyploidy and liver proliferation: central role of insulin signaling. Cell Cycle 2010;9:460-466.
35. Celton-Morizur S, Desdouets C. Polyploidization of liver cells. Adv Exp Med Biol 2010;676:123-135.
36. Savic D, Ramaker RC, Roberts BS, Dean EC, Burwell TC, Meadows SK, Cooper SJ, et al. Distinct gene regulatory programs define the inhibitory effects of liver X receptors and PPARG on cancer cell proliferation. Genome Med 2016;8:74.

37. Sporn MB, Suh N, Mangelsdorf DJ. Prospects for prevention and treatment of cancer with selective PPARgamma modulators (SPARMs). Trends Mol Med 2001;7:395-400.
38. Lin CY, Vedin LL, Steffensen KR. The emerging roles of liver X receptors and their ligands in cancer. Expert Opin Ther Targets 2016;20:61-71.
39. Chuu CP, Kokontis JM, Hiipakka RA, Liao S. Modulation of liver X receptor signaling as novel therapy for prostate cancer. J Biomed Sci 2007;14:543-553.
40. Pascual-Garcia M, Carbo JM, Leon T, Matalonga J, Out R, Van Berkel T, Sarrias MR, et al. Liver X receptors inhibit macrophage proliferation through downregulation of cyclins D1 and B1 and cyclin-dependent kinases 2 and 4. J Immunol 2011;186:4656-4667.
41. Li S, Chen X, Zhou L, Wang BM. Farnesoid X receptor signal is involved in deoxycholic acid-induced intestinal metaplasia of normal human gastric epithelial cells. Oncol Rep 2015;34:2674-2682.
42. Xu Y, Watanabe T, Tanigawa T, Machida H, Okazaki H, Yamagami H, Watanabe K, et al. Bile acids induce cdx2 expression through the farnesoid x receptor in gastric epithelial cells. J Clin Biochem Nutr 2010;46:81-86.
43. Zhou H, Ni Z, Li T, Su L, Zhang L, Liu N, Shi Y. Activation of FXR promotes intestinal metaplasia of gastric cells via SHP-dependent upregulation of the expression of CDX2. Oncol Lett 2018;15:7617-7624.
44. Wang YD, Chen WD, Moore DD, Huang W. FXR: a metabolic regulator and cell protector. Cell Res 2008;18:1087-1095.
45. Zhang Y, Gong W, Dai S, Huang G, Shen X, Gao M, Xu Z, et al. Downregulation of human farnesoid X receptor by miR-421 promotes proliferation and migration of hepatocellular carcinoma cells. Mol Cancer Res 2012;10:516-522.
46. Geier A, Trautwein C. Bile acids are "homeotrophic" sensors of the functional hepatic capacity and regulate adaptive growth during liver regeneration. Hepatology 2007;45:251-253.
47. Wang YD, Chen WD, Wang M, Yu D, Forman BM, Huang W. Farnesoid X receptor antagonizes nuclear factor kappaB in hepatic inflammatory response. Hepatology 2008;48:1632-1643.
48. Celton-Morizur S, Merlen G, Couton D, Margall-Ducos G, Desdouets C. The insulin/Akt pathway controls a specific cell division program that leads to generation of binucleated tetraploid liver cells in rodents. J Clin Invest 2009;119:1880-1887.
49. Fujiwara T, Bandi M, Nitta M, Ivanova EV, Bronson RT, Pellman D. Cytokinesis failure generating tetraploids promotes tumorigenesis in p53-null cells. Nature 2005;437:1043-1047.

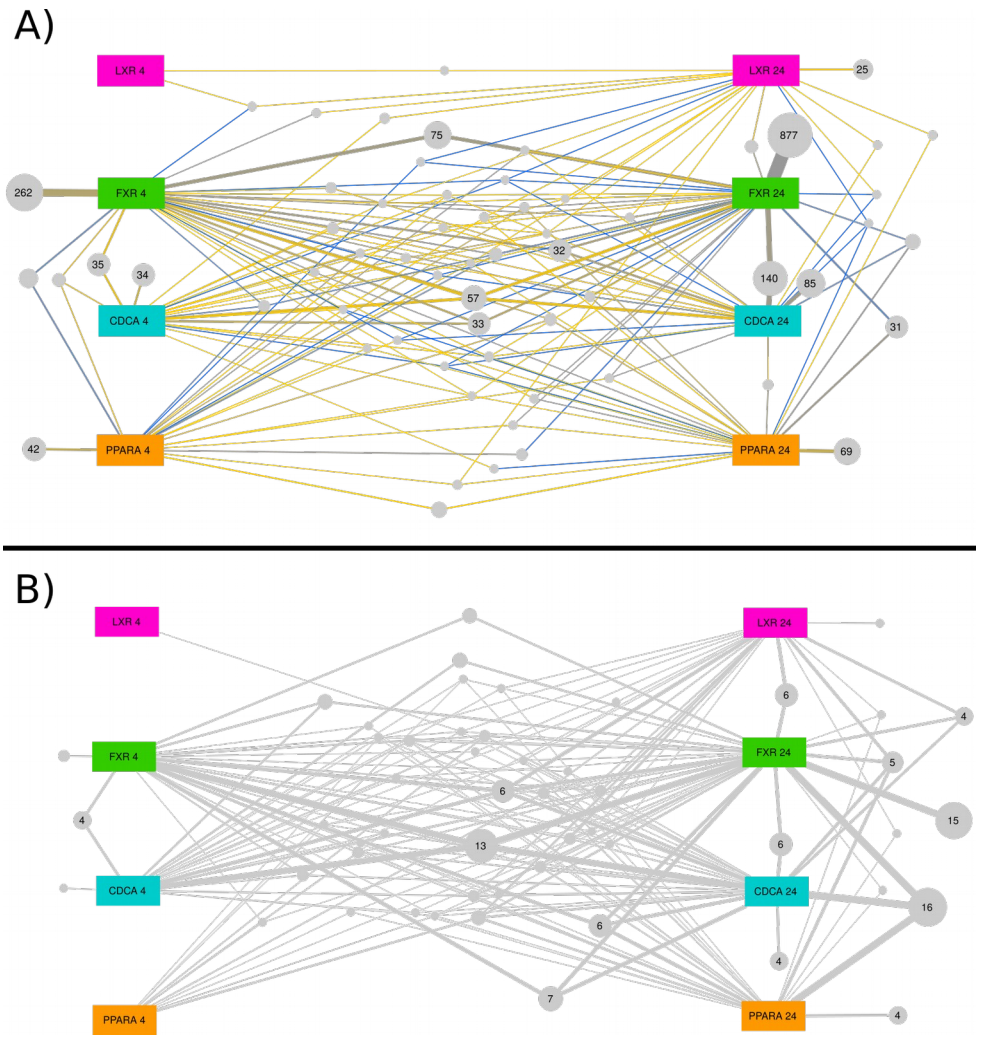

Figure 1: Visual Representation of the specific and shared effects of the treatments. Large coloured nodes denote the 4 treatments at 4h (on the left) or at 24h (on the right), while grey bubbles denote groups of regulated genes (panel A) or of enriched pathways (panel B), which are associated to the same set of treatments. For example, panel A shows that 1214 genes are regulated only by FXR-L: 262 only after 4h, 75 at both timepoints and 877 only at 24h. Similarly, the center bubble indicates that 57 genes are regulated by both FXR-L and CDCA at both timepoints. The size of the bubbles and of the connections with their associated treatments is proportional to the number of genes or pathways in the group. In panel A, the color of the connection further indicates the ratio between genes which are activated (yellow) or inhibited (blue) by this treatment. The original cytoscape files are available as supplementary material and a summary of the observed overlap is available in Table 1.

Figure 2: Effect of FXR-L and LXR-L treatments on genes associated to the cell-cycle pathway. These heatmaps show the expression levels of genes driving the cell-cycle pathway at 24h for the FXR-L (on the left) and LXR-L (on the right) treatments compared to the controls (non-treated (NT) and DMSO-treated) according to GSEA (see methods and supplementary material). For each gene, the 9 experimental values are centered around their mean (in grey). Larger values appear in yellow, while lower values are blue. Each heatmap has an extra column on the right showing the tendency of the common genes for the other treatment. With FXR-L treatment, most genes are up-regulated, while they are down-regulated with LXR-L. Among the 27 genes regulated by the two treatments, only 3 have the same profile in the two conditions (TGFB3, ORC3L and CCND1).

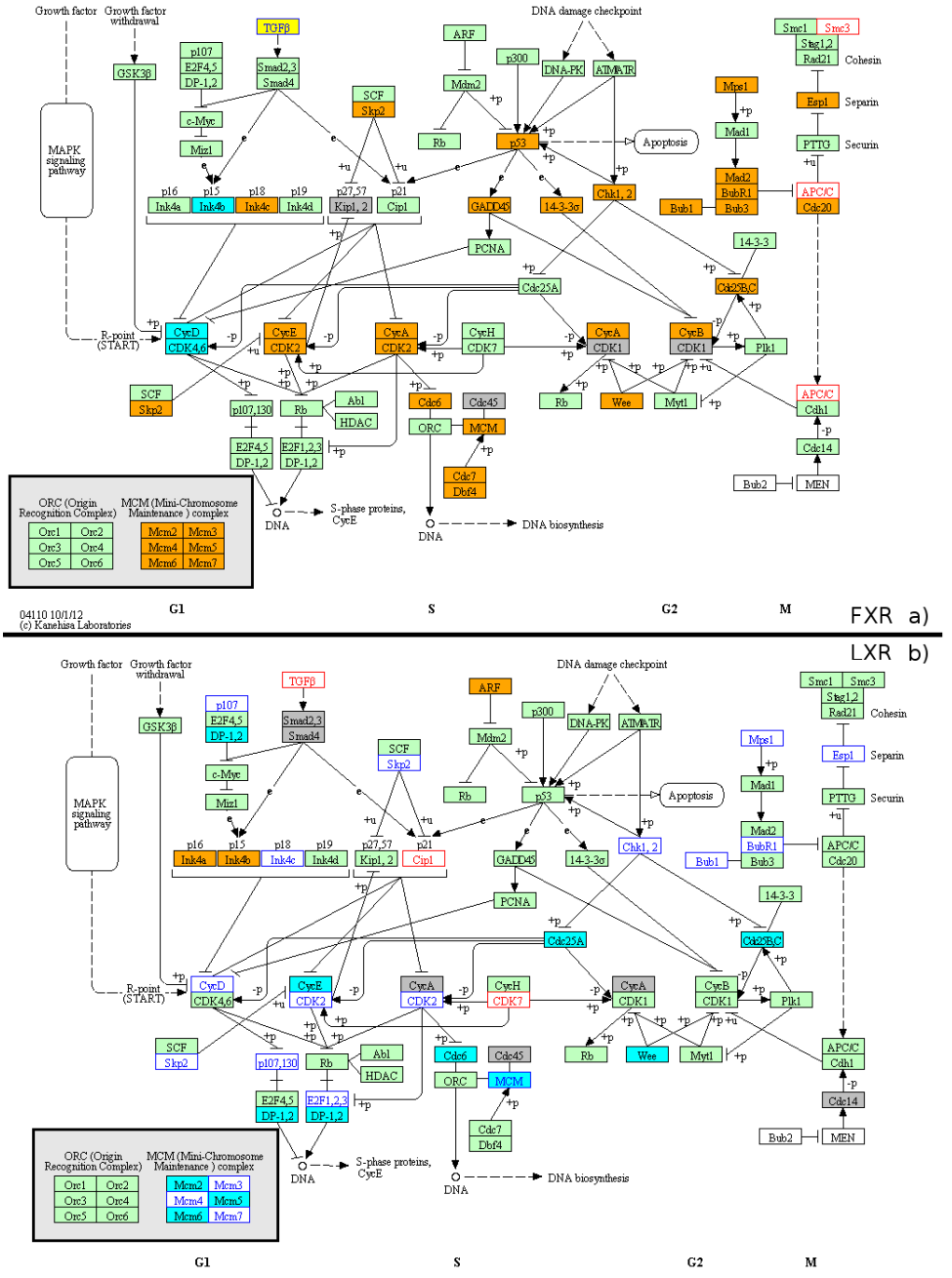

Figure 3: Visualisation of the effects of FXR-L and LXR-L on the KEGG cell cycle pathway map. Genes found in the leading edge of the cell cycle pathway at 24h after FXR-L (panel A) and LXR-L (panel B) treatments are highlighted. Boxes with a blue (resp. orange) background denote down-regulated (resp. up-regulated) genes (|log foldchange| > 1.2). White boxes with blue (resp. red) text denote smaller down-regulations (resp. up-regulations). The yellow TGFβ box in panel A corresponds to the TGFβ1, TGFβ2 and TGFβ3 genes which are regulated in opposite directions.

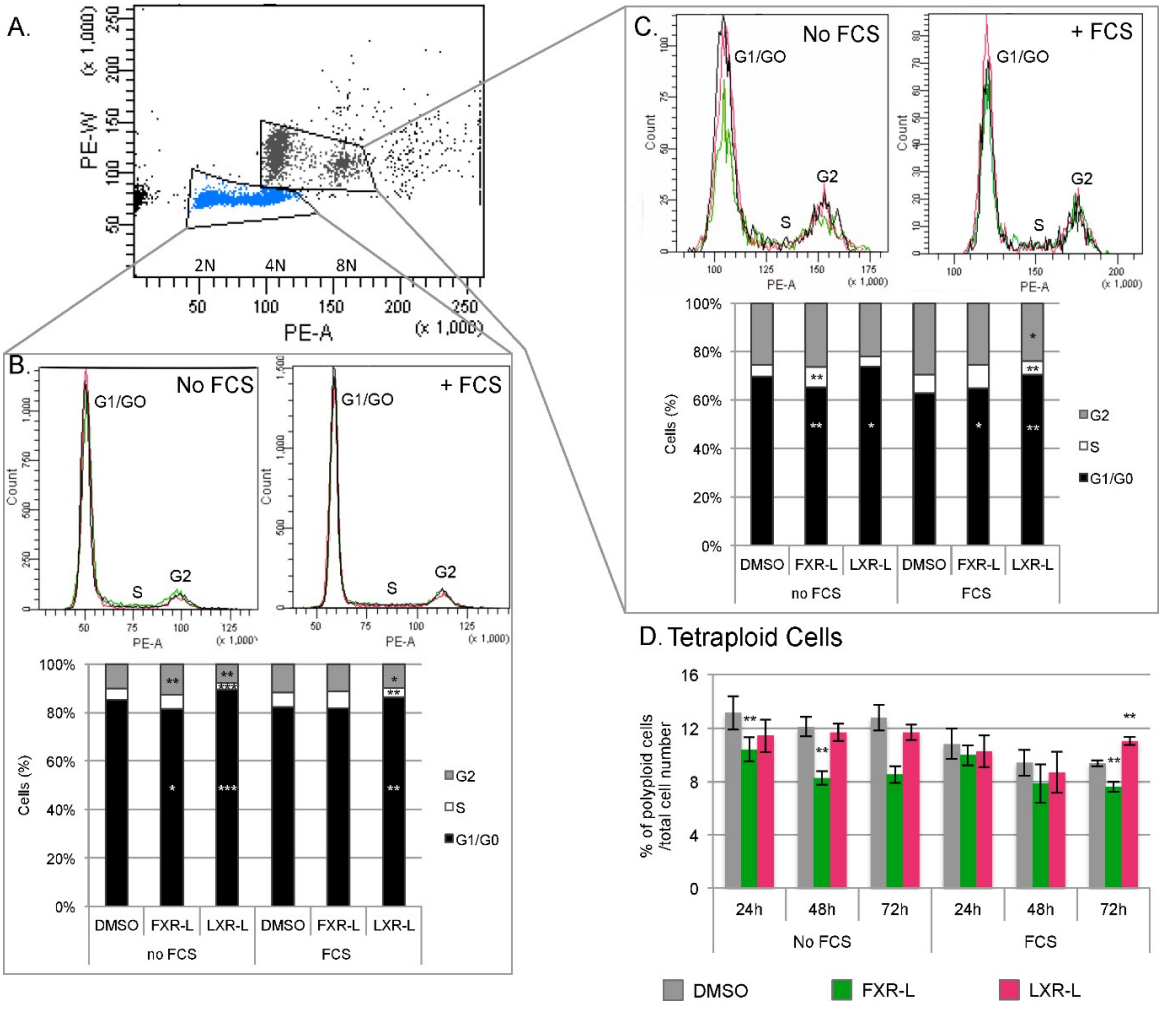

Figure 4: FXR and LXR affect the cell progression and the ploidy of HepaRG cells. The cell cycle distribution and the ploidy were analyzed by PI staining and FACS. A. The panel shows the group of HepaRG cells, the diploid cells (2N) and tetraploid cells (4N), B and C. The panels and the graphs show the cell cycle distribution at 72h of treatment with DMSO, FXR-L 1 uM or LXR-L 2 uM. D. The graph shows the percentage of tetraploid cells at 24h, 48h and 72h with the different treatments. * : p-value < 0.05, ** < 0.01, *** < 0.001 versus DMSO (Student's t test). N=8.

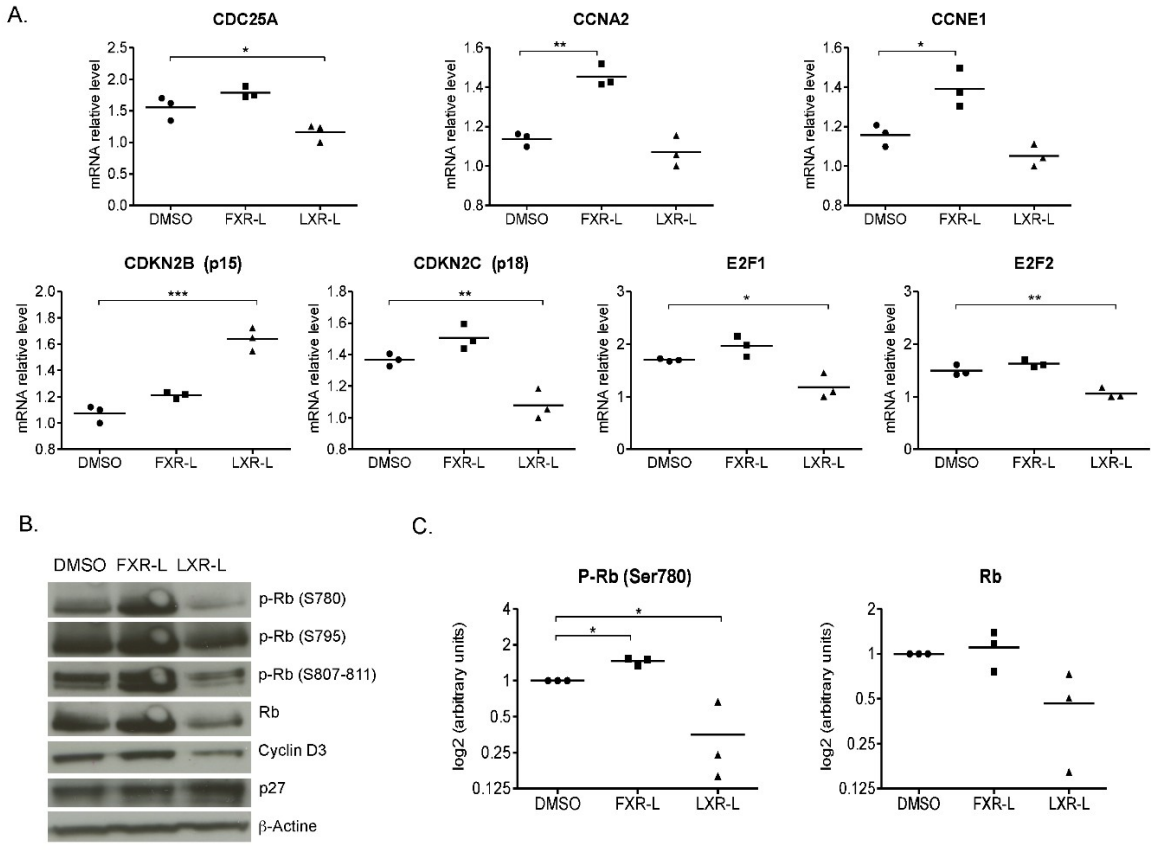

Figure 5: Validation of the effects of FXR and LXR on cell cycle regulators by RT-qPCR (A) and Western blot (B). HepaRG cells have been treated 24h in the same condition as for the microarrays (same ligands and DMSO as control). A. Relative mRNA levels for genes regulated in the microarray data. B. Representative Western blot of Rb, phospho-Rb, Cyclin D3, and p27 in whole HepaRG cell lysates. C. densitometric quantification of phospho-Rb and Rb. * : p-value < 0.05, ** < 0.01 versus DMSO (Student's t test). N=3.

		Genes		KEGG Pathways	
		#	%	#	%
All ligands combined	4h	407	20.35	7	4.58
	24h	1264	63.20	64	41.83
	4h and 24h	329	16.45	82	53.59
	Total	2000		153	
CDCA-L	alone	119	23.02	5	4.39
	shared with FXR-L	318	61.51	40	35.09
	shared with LXR-L	7	1.35	1	0.88
s	shared with PPARA-L	6	1.16	0	0.00
	shared with multiple	67	12.96	68	59.65
	Total	517	100.00	114	100.00
FXR-L	alone	1214	71.08	20	14.29
	shared with CDCA	318	18.62	40	28.57
	shared with LXR-L	14	0.82	7	5.00
	shared with PPARA-L	91	5.33	4	2.86
	shared with multiple	71	75.23	69	63.57
	Total	1708	100.00	140	100.00
LXR-L	alone	26	38.81	1	2.17
	shared with CDCA	7	10.45	1	2.17
	shared with FXR-L	14	20.90	7	15.22
	shared with PPARA-L	6	8.96	1	2.17
	shared with multiple	14	59.70	36	80.43
	Total	67	100.00	46	100.00
PPARA-L	alone	127	43.05	4	6.45
	shared with CDCA	6	2.03	0	0.00
	shared with FXR-L	91	30.85	4	6.45
	shared with LXR-L	6	2.03	1	1.61
	shared with multiple	65	22.03	53	85.48
	Total	295	100.00	62	100.00

Table 1: Summary of the distribution of differentially expressed (DE) genes and enriched pathways among time points and treatments. Top four rows: number and percentage of DE genes and positively enriched KEGG pathways from all treatments combined, found either at a single time point (4h, 24h) or at both time points (4h and 24h); totals from both time points. Remaining table: Numbers and percentages found per ligand treatment (at any or both time points), with a breakdown of how many DE genes and enriched pathways are exclusive to one treatment and how many are shared between two or multiple treatments. This summary shows that cross-talks observed at the pathway level are not visible when looking solely at differentially expressed genes.

		KEGG Pathways: Metabolism		KEGG Pathways: Cell Growth		KEGG Pathways: Immune		KEGG Pathways: Others	
		#	%	#	%	#	%	#	%
	4h	3	4.17	1	2.08	3	13.04	0	0.00
	24h	38	52.78	17	35.42	7	30.43	2	20.00
	4h and 24h	31	43.06	30	62.50	13	56.52	8	80.00
	Total	72	100.00	48	100.00	23	100.00	10	100.00
CDCA-L	alone	1	1.85	3	8.11	1	6.67	0	0.00
	shared with FXR-L	9	16.67	14	37.84	10	66.67	7	87.50
	shared with LXR-L	1	1.85	0	0.00	0	0.00	0	0.00
	shared with PPARa-L	0	0.00	0	0.00	0	0.00	0	0.00
	shared with multiple	43	79.63	20	54.05	4	26.67	1	12.50
	Total	54	100.00	37	100.00	15	100.00	8	100.00
FXR-L	alone	6	9.23	7	15.91	6	28.57	1	10.00
	shared with CDCA	9	13.85	14	31.82	10	47.62	7	70.00
	shared with LXR-L	3	4.62	3	6.82	1	4.76	0	0.00
	shared with PPARa-L	3	4.62	0	0.00	0	0.00	1	10.00
	shared with multiple	44	67.69	20	45.45	4	19.05	1	10.00
	Total	65	100.00	44	100.00	21	100.00	10	100.00
LXR-L	alone	1	3.45	0	0.00	0	0.00	0	N/A
	shared with CDCA	1	3.45	0	0.00	0	0.00	0	N/A
	shared with FXR-L	3	10.34	3	20.00	1	50.00	0	N/A
	shared with PPARa-L	1	3.45	0	0.00	0	0.00	0	N/A
	shared with multiple	23	79.31	12	80.00	1	50.00	0	N/A
	Total	29	100.00	15	100.00	2	100.00	0	N/A
PPARA-L	alone	2	4.26	1	11.11	1	25.00	0	0.00
	shared with CDCA	0	0.00	0	0.00	0	0.00	1	50.00
	shared with FXR-L	3	6.38	0	0.00	0	0.00	0	0.00
	shared with LXR-L	1	2.13	0	0.00	0	0.00	0	0.00
	shared with multiple	41	87.23	8	88.89	3	75.00	1	50.00
	Total	47	100.00	9	100.00	4	100.00	2	100.00
CDCA, FXR-L (merged)	alone	16	32.65	24	51.06	17	77.27	8	80.00
	shared with LXR-L	8	16.33	15	31.91	2	9.09	0	0.00
	shared with PPARa-L	25	51.02	8	17.02	3	13.64	2	20.00
	Total	49	100.00	47	100.00	22	100.00	10	100.00

Table 2: Distribution of categories of enriched pathways depending on their association with treatments. Enriched KEGG pathways were grouped manually into 4 wide categories ("Metabolism", "Cell growth and death", "Immune system" and "Other"). Top four rows: Number and percentage of positively enriched KEGG pathways from all treatments combined, found either at a single time point (4h, 24h) or at both time points (4h and 24h) in each category; totals from both time points. Remaining table: Numbers and percentages of pathways found per ligand treatment (at any or both time points), with a breakdown of how many DE genes and enriched pathways are exclusive to one treatment and how many are shared between two or multiple treatments. Bottom section: Numbers and percentages of pathways found if the pathways lists from CDCA and FXR-L treatments are merged.